Neuroradiology
https://doi.org/10.1007/s00234-025-03794-9

RESEARCH

Age-related changes in cerebral blood flow and arterial transit time in children: insights from single- and multi-delay ASL

Yeva Prysiazhniuk[1,2] · Rui Duarte Armindo[3] · Sasha Alexander[4] · Michael Moseley[5] · Kristen W. Yeom[4] · Jakub Otáhal[1] · Martin Kynčl[2] · Elizabeth Tong[5] · Jan Petr[6,7] · Moss Y. Zhao[4] · Gary K. Steinberg[4]

Received: 26 March 2025 / Accepted: 20 September 2025

Abstract

Background Arterial spin labeling (ASL) MRI is a non-invasive perfusion imaging technique with potential for assessing hemodynamics in children. However, understanding hemodynamic changes in developing brains remains challenging. This study investigates the impact of normal brain development on ASL-derived cerebral blood flow (CBF) and arterial transit time (ATT) in MR-negative children.

Methods Thirty-two pediatric subjects (ages 0.7–17.9 years, mean 9.3 ± 5.3y, 19 male) with MR-negative findings were retrospectively included. Four pseudo-continuous ASL (PCASL) scans were acquired: single-delay (PLD 1525 or 2025 ms) and multi-delay (3 or 7 delays). CBF and ATT in supratentorial gray matter (GM), white matter (WM), and total-brain (TB) regions were analyzed using paired t-tests, Cohen's d, Spearman correlation, and mixed linear regression models.

Results Single-delay CBF was significantly higher than 3-delay CBF in GM and WM ($p < 0.001$ PLD 2025 ms; $p = 0.02$ PLD 1525 ms). WM and TB CBF correlated negatively with age (rho=-0.56, $p < 0.001$), whereas GM CBF showed no significant correlation (rho=-0.03, $p = 0.87$); the trends differed significantly ($p = 0.01$). GM and TB ATT increased with age ($r^2 > 0.11$, $p < 0.021$). WM and TB CBF correlated with WM and combined WM/GM volumes (rho=-0.42, $p = 0.02$; rho=-0.46, $p = 0.008$).

Conclusion GM and WM exhibit distinct age-related hemodynamic patterns. WM perfusion declines with age and correlates with WM volume, while GM perfusion remains stable. The progressive increase in GM ATT highlights the need for cautious interpretation of single-delay ASL data in pediatric studies.

Keywords Perfusion · ASL · Pediatric · Brain Development · Arterial Transit Time

Introduction

Metabolic demands in the developing brain change in the early years, yet age-related hemodynamic changes in infants and children remain understudied. Maintaining adequate cerebral blood flow (CBF) is essential for delivering oxygen and nutrients to the brain while removing metabolic waste, making CBF a critical parameter in brain physiology [1]. Various modalities exist for measuring CBF, including [^{15}O]H_2O positron emission tomography (PET), Xenon-133 single photon emission computed tomography (SPECT), and several magnetic resonance imaging (MRI) perfusion methods such as Dynamic Susceptibility Contrast (DSC), Dynamic Contrast Enhanced (DCE), and Arterial Spin Labeling (ASL). However, concerns about radiation exposure and the safety of exogenous contrast agents [2] have limited the use of PET, SPECT, and dynamic gadolinium-dependent MRI in pediatric populations. This has increased interest in using ASL as a safer alternative for pediatric neuroimaging. ASL stands out as the only method that allows regional CBF quantification without the need for exogenous contrast agents, making it optimal for routine perfusion scanning, especially in clinical groups at risk. ASL offers additional advantages such as more straightforward clinical

Can Jan Petr, Moss Y. Zhao, and Gary K. Steinberg as co-senior Authors

Extended author information available on the last page of the article

Published online: 07 October 2025

implementation, applicability to preterm infants and neonates, and suitability for longitudinal studies as it allows absolute CBF quantification [3].

Several review articles have emphasized the need to adapt pediatric protocols from adult standards, noting the importance of accounting for greater age-related variability in CBF and arterial transit time (ATT) in developing brains [4, 5]. They have highlighted the emerging relevance of advanced ASL techniques, such as Hadamard-encoded and multi-delay methods, to better understand and standardize perfusion measurements in pediatric populations [6]. While previous studies have investigated CBF variance in pre-adolescent and adolescent cohorts, age-related changes in ATT still need to be studied [7, 8]. ATT is defined as the duration for the tagged blood to flow from the labeling region to the brain tissue. Our insufficient understanding of hemodynamic changes in the developing brain represents a significant challenge to the precise quantification of CBF and ATT maps in typical subjects and patients with brain diseases. Moreover, understanding age-related changes in different brain regions is crucial for accurate ASL interpretation in pediatric populations [9].

This study examines CBF and ATT changes measured by single- and multi-delay ASL in 32 typically-developing pediatric subjects. We compare CBF and ATT in supratentorial gray matter, white matter, and total brain regions (GM, WM, and TB, respectively) and their correlations with age. Additionally, we explore the association between regional CBF and age with brain volumetric changes.

Materials and methods

This retrospective study included 32 pediatric subjects (19 males, aged 0.7–17.9 years, mean ± SD: 9.3 ± 5.3 years) who underwent routine MRI examination between July 2021 and March 2022 at Lucile Packard Children's Hospital Stanford. The protocol included ASL as part of the diagnostic setup to assess cerebral perfusion. Additional ASL sequences were included within the same scanning session when increased scanning capacities were available. Inclusion criteria were: age under 18 years, MR-negative status (defined as the absence of structural or functional abnormalities), and availability of single- and multi-delay ASL data. MR-negative status was confirmed by an experienced pediatric neuroradiologist (ET, 7 years of expertise) based on the structural imaging scans and sedation data were retrieved from the database. The study received ethics approval from Stanford IRB's Administrative Panel on Human Subjects in Medical Research (IRB-72827). Written informed consent for secondary data use in the present study was obtained from the parents or guardians of all participants, in accordance with the Declaration of Helsinki [10].

MRI data was acquired on a 3 T GE Premier (GE Healthcare, Milwaukee, USA) with a 21-channel head and neck coil. All included subjects underwent T1-weighted (3D SPGR, TR/TE 6.8/2.9 ms, flip angle 15°, voxel size isometric 1 mm^3) and T2-weighted (2D FSE, TR/TE 4882/103.2 ms, flip angle 111°, voxel size $0.5 \times 0.5 \times 2.5$ mm^3) scans. Four types of background-suppressed pseudo-continuous ASL (PCASL) scans were obtained: single-delay $PCASL_{PLD2025}$ (labeling duration (LD) 1450 ms, post-labeling delay (PLD) 2025 ms) and $PCASL_{PLD1525}$ (LD 1450 ms, PLD 1525 ms), as well as multi-delay $PCASL_{7PLD}$ (LD 550 ms, PLDs 700, 1250, 1800, 2350, 2900, 3450, and 4000 ms) and $PCASL_{3PLD}$ (LD 1700 ms, PLDs 300, 2000, and 3700 ms). Further details of the MRI acquisition protocol are provided in Table 1. A sensitivity analysis was performed to assess potential differences in age, sex, and sedation among populations scanned with the four modalities. ANOVA was used for the continuous variable (age), while chi-squared tests were applied to the categorical variables (sex and sedation status).

For multi-delay sequences, scanner-reconstructed arterial-time (AT)-corrected and uncorrected CBF, as well as ATT maps were extracted [11]. For single-delay PCASL, only scanner-reconstructed, uncorrected CBF was retrieved. Image processing, including T1-weighted segmentation, spatial normalization, and population-level analysis, was performed using ExploreASL v1.12 [12]. ASL data quality was assessed independently by two researchers with 10+ and 3 years of ASL experience (JP, YP) according to the previously described methodology [13]. Scans were categorized as "good" (well-distributed gray matter perfusion signal without motion or labeling.

artifacts), "acceptable" (minor motion or macrovascular artifacts causing regional signal loss), or "vascular" (dominant macrovascular artifact due to delayed arterial arrival). Mean CBF and ATT values in supratentorial GM, deep WM, and TB (supratentorial GM and WM) regions were extracted in native space using CAT12 [14]; examples of ROI selection are shown in Supplementary Fig. 1. Additionally, absolute volumes and volumes relative to intracranial volume (ICV) were extracted for GM and WM.

Statistical analysis

Statistical analyses and visualizations were performed using R statistical software (version 4.3.0; R Foundation for Statistical Computing, Vienna, Austria. https://www.R-project.org/). Paired t-tests and Cohen's d with Hedge's correction were applied to compare mean CBF and ATT values across GM,

Table 1 MRI acquisition parameters of structural and perfusion data

	$PCASL_{7PLD}$ ($n=18$)	$PCASL_{3PLD}$ ($n=32$)	$PCASL_{2025ms}$ ($n=19$)	$PCASL_{1525ms}$ ($n=10$)
Labeling and Readout	3D PCASL FSE stack-of-spiral	3D PCASL FSE stack-of-spiral	3D PCASL FSE stack-of-spiral	3D PCASL FSE stack-of-spiral
FOV	240 mm	240 mm	240 mm	240 mm
Acquired resolution	512 points/4 arms	512 points/8 or 4 arms	512 points/8 arms	512 points/8 arms
Slice thickness/spacing between slices mm	3/3	3/3	4/4	4/4
TR/TE ms, FA°	7100/23.2 ms, 111°	7100/23.2 ms, 111°	4890/52.9 ms, 111°	4680/52.9 ms, 111°
Number of excitations (NEX)	1	2	3	3
(Effective) LD	550 ms	1700 ms	1450 ms	1450 ms
PLD	700, 1250, 1800, 2350, 2900, 3450, 4000 ms	300, 2000, 3700 ms	2025 ms	1525 ms

Other parameters: M0 scan included, 4 background suppression pulses, labeling plane was fixed to 2 cm below the FOV without manual adjustment. Perfusion data acquisition parameters

T1w T1-weighted, *T2w* T2-weighted, *SPGR* spoiled gradient echo, *FSE* fast spin echo, *FOV* field of view, *PCASL* pseudo-continuous ASL, *TR* repetition time, *TE* echo time, *FA* flip angle, *LD* labeling duration, *PLD* post labeling delay, *M0* equilibrium magnetization, *BS* background suppression

WM, and TB between ASL variants. Specifically, CBF values from $PCASL_{2025ms}$, $PCASL_{1525ms}$, and $PCASL_{ATC-7PLD}$ were compared to those from $PCASL_{ATC-3PLD}$ due to the larger sample sizes of the overlapping datasets. To assess the effect of AT-correction on absolute CBF quantification, both corrected and uncorrected CBF values from $PCASL_{3PLD}$ and $PCASL_{7PLD}$ sequences were analyzed. Student t-tests were used to assess the impact of sex and sedation on GM $CBF_{ATC-3PLD}$.

A Spearman correlation was employed to investigate the relationship between age and AT-corrected or uncorrected CBF values in GM, WM, and TB for the $PCASL_{3PLD}$ and $PCASL_{7PLD}$ sequences. Differences in correlation strength across GM, WM, and TB were assessed using a combined linear regression model, with the significance of the interaction term indicating differences between the linear models. The differences in the correlation between GM $CBF_{ATC-3PLD}$ and age across sedated/non-sedated and male/female subpopulations were evaluated using ANOVA tests applied to the corresponding linear regression models. A two-parameter linear regression model was estimated using both $PCASL_{3PLD}$ and $PCASL_{7PLD}$ ATT and age in GM, WM, and TB, with the acquisition approach included as a separate parameter. The significance of the models was evaluated using ANOVA, and r^2 was reported as the correlation coefficient. Voxel-wise Spearman correlation analyses of $PCASL_{3PLD}$ ATT and CBF with age were performed, incorporating false discovery rate (FDR) correction and cluster correction to visualize the regional effects.

A Spearman correlation was used to compare regional CBF (GM, WM, TB), regional volumes (GM, WM, and combined GM and WM, respectively), and age. Volumetric markers included absolute regional volumes and regional volumes relative to the absolute intracranial volume. Voxel-wise quantification of population mean $PCASL_{ATC-3PLD}$ CBF and ATT maps was performed alongside the voxel-wise population coefficient of variation (CoV) for $PCASL_{ATC-3PLD}$ CBF and ATT, defined as the ratio of the voxel-wise standard deviation to the voxel-wise mean. A statistical significance threshold of $p < 0.05$ was applied, with a family-wise error rate (FWER) correction using the Holm method implemented throughout the study [15].

Results

All subjects had $PCASL_{3PLD}$ acquired. 81 scans were obtained, of which 86.4% were classified as good, 12.3% as acceptable, and 1.2% exhibited vascular features; no scans were excluded due to poor quality. Figure 1 provides an overview of the experimental data, and Fig. 2; Table 2 describe the CBF and ATT distributions across ROIs and PCASL variants. More detailed information on the distribution of sex, sedation status, and clinical indication is provided in Supplementary Table 1. The sensitivity analysis did not reveal any significant differences in age, sex, or sedation among subjects scanned with the four methods (Supplementary Table 2).

Hemodynamic parameters in multi-delay ASL

No significant difference was observed in ATT between $PCASL_{3PLD}$ and $PCASL_{7PLD}$ ($p>0.51$) (Table 3). In $PCASL_{3PLD}$, ATT was significantly higher in WM compared

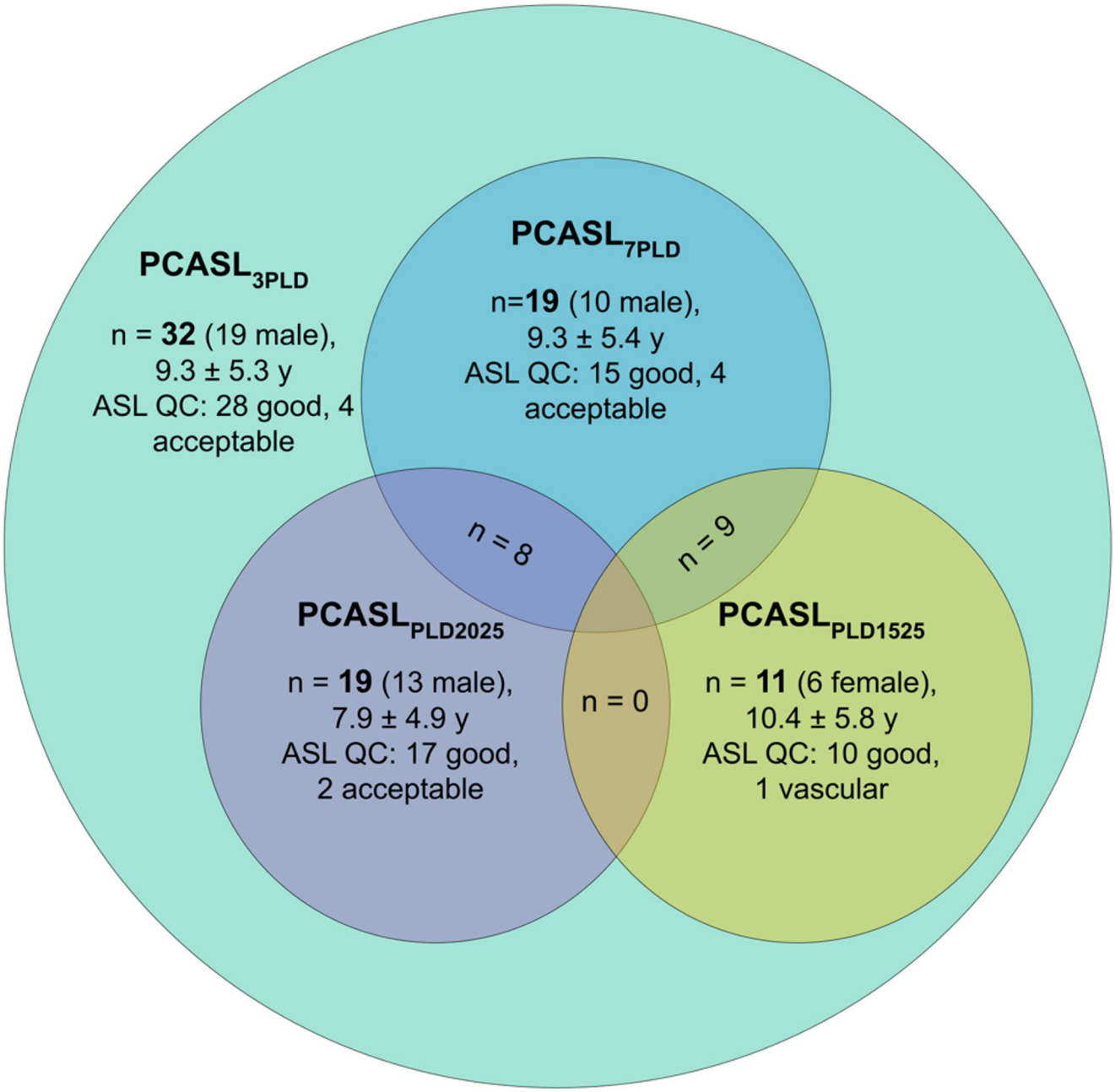

Fig. 1 Venn diagram of analyzed datasets. "n" indicates the sample sizes, and age is presented as mean ± standard deviation

to GM ($p=0.004$, d = 0.29) and higher in WM compared to TB ($p=0.005$, d = 0.28). In $PCASL_{7PLD}$, ATT was also significantly higher in WM than in GM and TB ($p<0.001$, d = 0.63 and $p<0.001$, d = 0.56, respectively).

In GM, AT-correction significantly increased $PCASL_{3PLD}$ GM-CBF by 11.6% while having no significant effect on $PCASL_{7PLD}$ GM-CBF. In WM, AT-correction did not impact $PCASL_{3PLD}$ WM-CBF but significantly increased it in $PCASL_{7PLD}$ by 10.2%. For TB, AT-correction significantly raised $PCASL_{3PLD}$ TB-CBF by 10.1% on average, with no notable effect on TB-CBF in $PCASL_{7PLD}$. After AT-correction, there was no significant difference between $PCASL_{ATC-3PLD}$ and $PCASL_{ATC-7PLD}$ TB-CBF. Therefore, we will use $PCASL_{ATC-3PLD}$ as a reference for multi-delay parameters in further analysis. No significant differences in GM $CBF_{ATC-3PLD}$ were observed between male and female or between sedated and non-sedated participants ($p=0.78$, d = 0.11; $p=0.47$, d = 0.25, respectively). Overall,

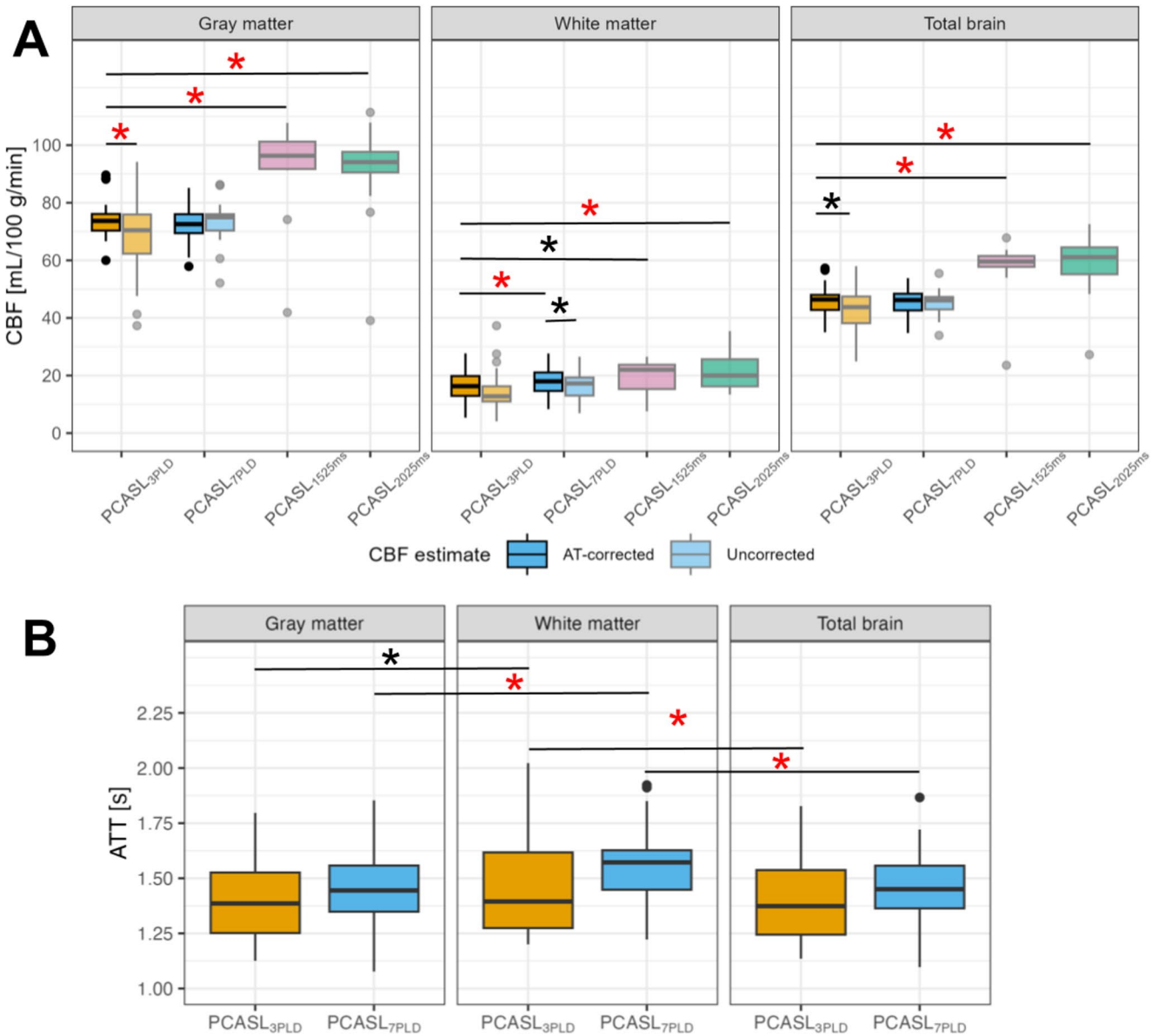

Fig. 2 (**A**) Boxplots of CBF distributions in the TB, GM, and WM regions. (**B**) Boxplots of ATT distributions in the TB, GM, and WM regions. Red stars indicate significant differences with p-values < 0.05 after FWER correction. Black stars indicate significant differences with p-values < 0.05 before FWER correction

$PCASL_{ATC-3PLD}$ CBF in GM was significantly higher than in TB ($p < 0.001$, d = 4.7), and CBF in TB was significantly higher than in WM ($p < 0.001$, d = 5.7).

Comparison of regional multi- and single-delay ASL CBF

$PCASL_{PLD2025}$ GM-CBF and $PCASL_{PLD1525}$ GM-CBF were significantly higher than $PCASL_{ATC-3PLD}$ GM-CBF (Table 3). On average, $PCASL_{PLD2025}$ and $PCASL_{PLD1525}$ GM-CBF were 23.6% and 25.4% higher than $PCASL_{ATC-3PLD}$ GM-CBF. Similar trends in WM were observed; $PCASL_{PLD2025}$ WM-CBF and $PCASL_{PLD1525}$ WM-CBF were significantly higher than $PCASL_{ATC-3PLD}$ WM-CBF. On average, $PCASL_{PLD2025ms}$ and $PCASL_{PLD1525ms}$ WM-CBF were 24% and 31.7% higher than $PCASL_{ATC-3PLD}$ WM-CBF. Finally, in TB, there was again a significant difference between $PCASL_{PLD2025}$ TB-CBF and $PCASL_{PLD1525}$ TB-CBF compared to $PCASL_{ATC-3PLD}$ TB-CBF. On average, $PCASL_{PLD2025}$ and $PCASL_{PLD1525}$ TB-CBF were 24.6% and 30.2% higher than $PCASL_{ATC-3PLD}$ TB-CBF.

Table 2 Mean ± standard deviation of CBF and ATT in pediatric population

	$PCASL_{3PLD}$	$PCASL_{7PLD}$	$PCASL_{PLD2025}$	$PCASL_{PLD1525}$
Sample size	$n=32$	$n=19$	$n=19$	$n=10$
Uncorrected CBF [ml/100 g/min]				
GM CBF	68.3 ± 12.7	73.2 ± 8.0	91.9 ± 15.0	91.0 ± 19.8
WM CBF	13.5 ± 4.9	16.6 ± 5.0	21.8 ± 6.3	19.4 ± 5.9
TB CBF	42.7 ± 7.8	45.2 ± 4.7	58.8 ± 10.0	56.7 ± 12.2
AT-corrected CBF [ml/100 g/min]				
GM CBF	73.9 ± 6.2	72.3 ± 6.9	-	-
WM CBF	15.6 ± 4.5	17.8 ± 5.0	-	-
TB CBF	45.8 ± 5.2	45.2 ± 4.7	-	-
ATT [s]				
GM ATT	1.39 ± 0.18	1.44 ± 0.20	-	-
WM ATT	1.46 ± 0.22	1.57 ± 0.21	-	-
TB ATT	1.40 ± 0.19	1.45 ± 0.21	-	-

Table 3 Comparative analysis of CBF and ATT parameters between PCASL types, reported as cohen's d and p-values

ROI	$PCASL_{ATC-3PLD}$ vs. $PCASL_{PLD2025}$ CBF	$PCASL_{ATC-3PLD}$ vs. $PCASL_{PLD1525}$ CBF	$PCASL_{ATC-3PLD}$ vs. $PCASL_{ATC-7PLD}$ CBF	$PCASL_{ATC-3PLD}$ vs. $PCASL_{Uncorrected\_3PLD}$ CBF	$PCASL_{ATC-7PLD}$ vs. $PCASL_{Uncorrected\_7PLD}$ CBF	$PCASL_{ATC-3PLD}$ vs. $PCASL_{ATC-7PLD}$ ATT
GM	**d = 1.31, p < 0.001***	**d = 0.56, p = 0.004***	d = 0.15, p = 0.27	**d = 0.49, p = 0.004*,**	d = 0.11, p = 0.21	d < 0.1, p = 0.51
WM	**d = 0.61, p < 0.001***	**d = 0.67, p = 0.02**	**d = 0.52, p = 0.003**	d = 0.16, p = 0.29	**d = 0.32, p = 0.03**	d < 0.1, p = 0.62
TB	**d = 1.26, p < 0.001***	**d = 0.95, p = 0.002***	d < 0.1, p = 0.44	**d = 0.43, p = 0.01**	d < 0.1, p = 0.86	d < 0.1, p = 0.82

"" indicates p-values < 0.05 after FWER correction*

Hemodynamic trends in age

Figure 3 depicts the distribution of CBF across age, and Fig. 4 shows the distribution of ATT across age. The correlation analysis revealed a negative association between $PCASL_{ATC-3PLD}$ CBF and age in both WM and TB (rho = −0.56, $p < 0.001$ and rho = −0.56, $p < 0.001$, respectively), but no significant linear correlation in GM (rho = −0.03, $p = 0.87$). The combined model analysis demonstrated significant differences in the linear regression slopes between GM and TB ($p = 0.01$) and between GM and WM ($p = 0.01$). In the uncorrected $PCASL_{3PLD}$ and both AT-corrected and uncorrected $PCASL_{7PLD}$ sequences, no significant correlation with age was found across all ROIs, except for uncorrected $PCASL_{7PLD}$ CBF in TB (rho = −0.52, $p = 0.03$).

Furthermore, significant differences were identified in the linear regression models between AT-corrected and uncorrected CBF for both WM ($p = 0.02$) and TB ($p = 0.02$). No significant differences were observed when comparing the linear regression models between $PCASL_{ATC-7PLD}$ and $PCASL_{ATC-3PLD}$ CBF across GM, WM, and TB ($p = 0.85$, $p = 0.71$, $p = 0.95$, respectively). There was no significant difference between the linear models of the sedated and non-sedated populations ($p = 0.07$); however, a significant difference was observed between the linear models of female and male participants ($p = 0.002$) (Supplementary Fig. 2). GM and TB ATT showed a positive linear correlation with age ($r^2 = 0.12$, $p = 0.019$ and $r^2 = 0.11$, $p = 0.021$, respectively), but there was no significant correlation between WM ATT and age ($r^2 = 0.08$, $p = 0.075$) (Fig. 4).

The voxel-wise analysis results for the correlation between $PCASL_{ATC-3PLD}$ CBF and ATT with age are presented in Fig. 5. Regions with significant negative correlations between CBF and age were primarily localized in the WM and cerebellum. In contrast, regions with significant positive correlations between ATT and age were located in the cerebellum and GM.

Tissue volume trends across age

Figure 6 shows the correlation of absolute and relative GM and WM volumes with age, while Table 4 presents the correlation analysis results between volumetric parameters, age, and $PCASL_{3PLD}$ CBF. Relative GM volume (to ICV) correlated negatively with age, without a significant correlation with $PCASL_{3PLD}$ GM-CBF. In WM, $PCASL_{3PLD}$ WM-CBF correlated negatively with both absolute and relative WM volumes, while age correlated positively with both. For TB, there was a significant negative correlation between the

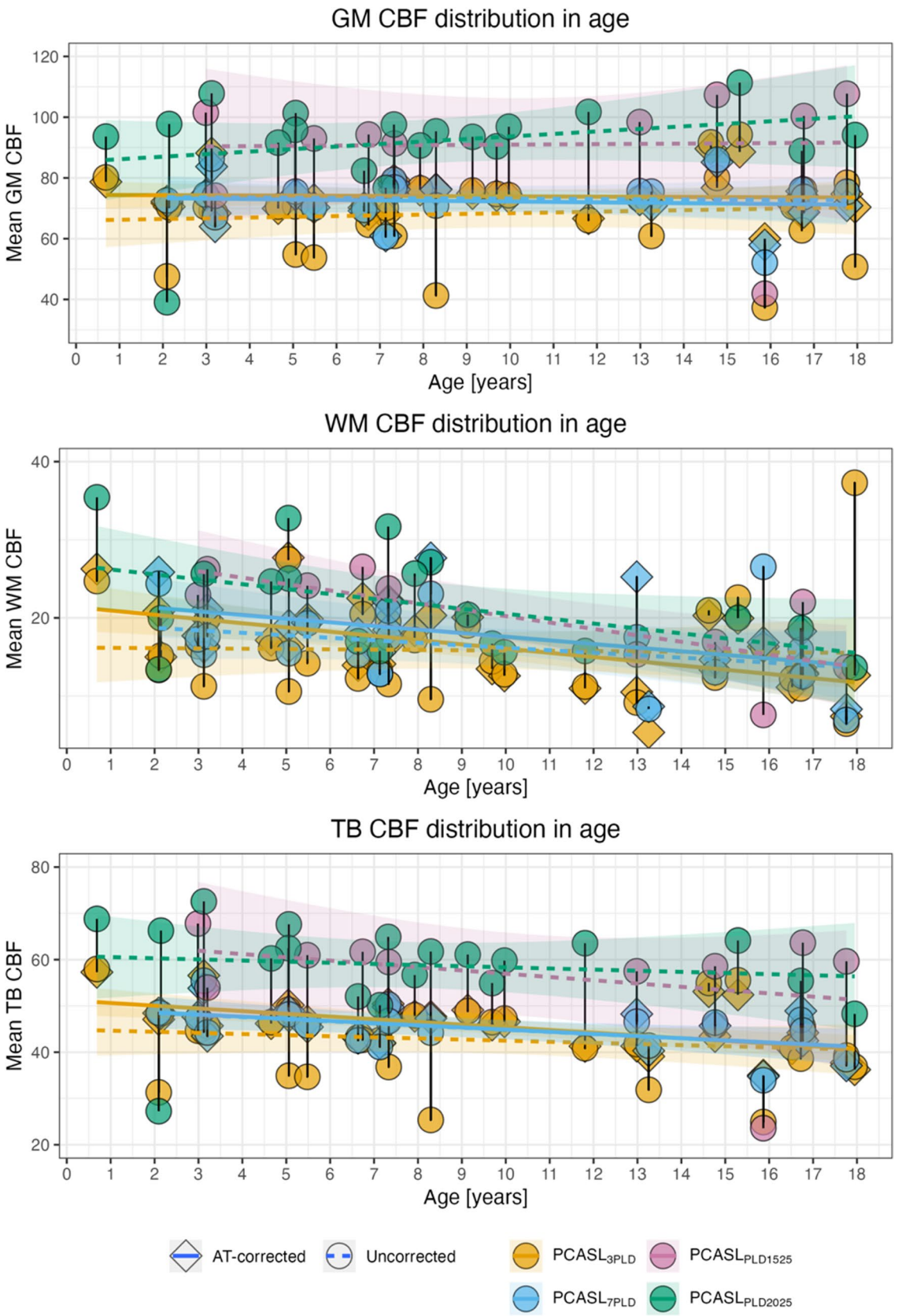

Fig. 3 Changes of cerebral perfusion with age. (**A**) GM CBF distribution in age. (**B**) WM CBF distribution with age. (**C**) TB CBF distribution with age

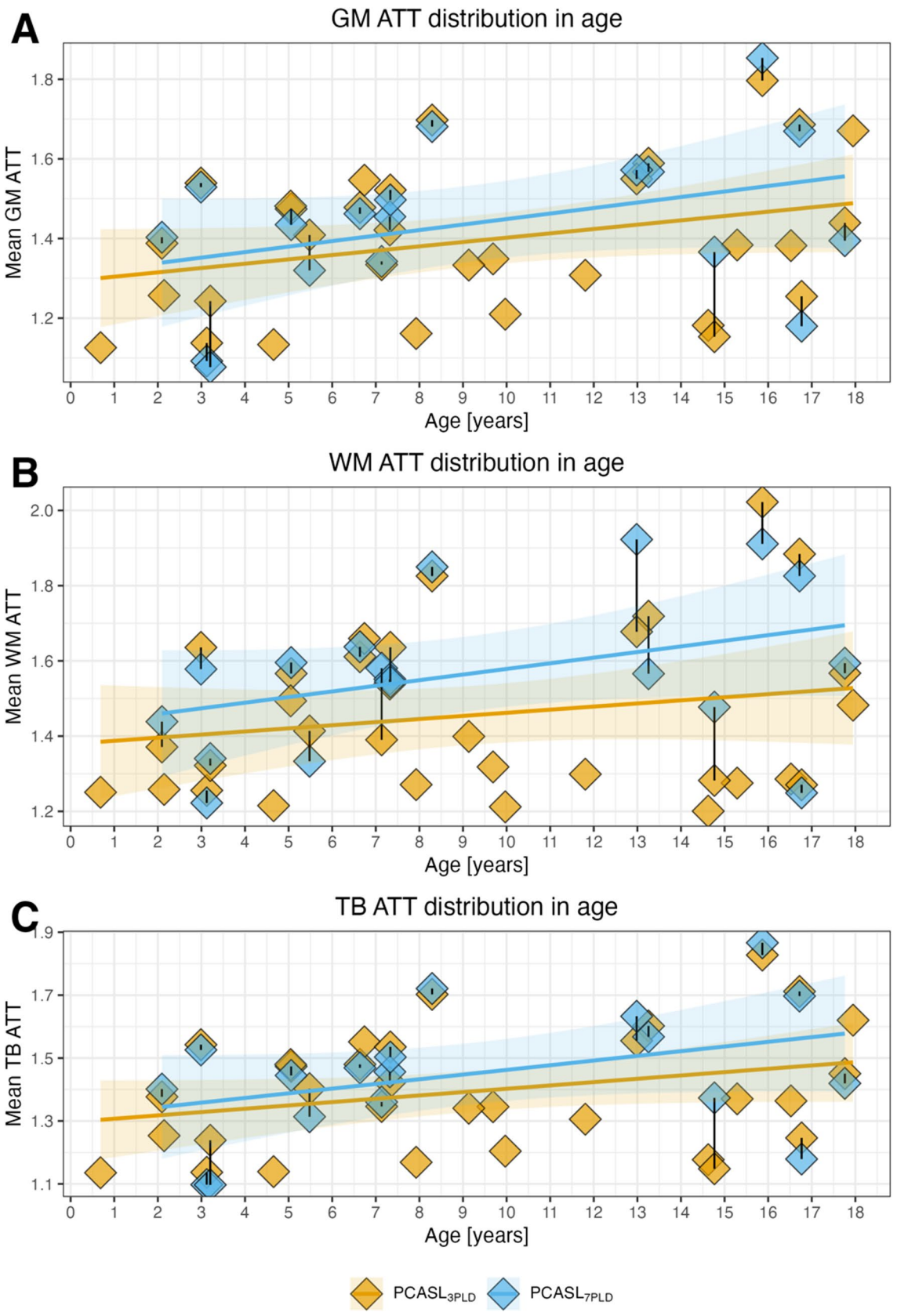

Fig. 4 Changes of hemodynamic parameters with age. (**A**) GM ATT distribution in age. (**B**) WM ATT distribution in age. (**C**) TB ATT distribution in age

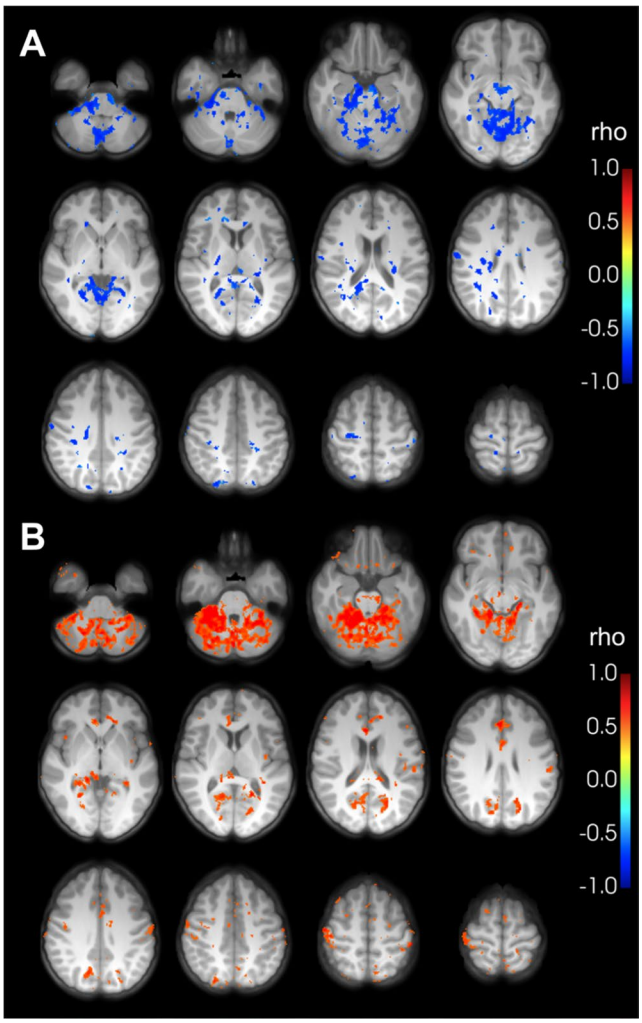

Fig. 5 Voxel-wise correlation between $PCASL_{3PLD}$ CBF (**A**) and ATT (**B**) with age, overlaid on the population T1-weighted image. Only voxels with statistically significant correlations (corrected for FWER) are displayed

absolute volume of combined GM and WM with $PCASL_{3PLD}$ TB-CBF and a positive correlation with age.

Hemodynamic variations in the pediatric population

Population mean CBF and ATT are visualized in Fig. 7. Population analysis of CoV (Supplementary Fig. 3) points out the increased variance of perfusion in WM and some deep GM structures such as the thalami and putamen.

Discussion

This study compared hemodynamic parameters derived from multi- and single-delay ASL in typically-developing children. Single-delay CBF was significantly higher than $PCASL_{3PLD}$ CBF, highlighting caution in interpreting absolute CBF quantification from single-delay ASL in children. Additionally, we analyzed age-related ATT and CBF trajectories in GM and WM to investigate physiologic hemodynamic changes and provide a basis for ASL protocol standardization in pediatric cohorts.

Despite comparable data quality control outcomes between single- and multi-delay datasets, significant differences in absolute CBF were observed, with multi-delay CBF values aligning more closely with results from other modalities [16]. These discrepancies may be attributed to factors such as: (i) scanner-specific post-processing algorithms, (ii) the consideration of longer PLDs in the multi-delay approach, and (iii) lower accuracy in CBF estimation linked with the single-delay approach [17, 18]. Furthermore, the magnitude of the difference between single- and multi-PLD ASL was dependent on the specific PLD selected for the single-delay acquisition, with longer PLDs generally yielding CBF values that were closer to those obtained with the multi-PLD approach. Notably, AT-correction also significantly affected absolute CBF values, likely due to reduced vascular artifacts [17], highlighting the crucial role of accounting for arterial transit time in accurately quantifying CBF through ASL methods. Although the recommended post-labeling delay for ASL in children is 1500 ms [3], our findings indicate that mean ATT in WM is higher than in GM, which is consistent with previous studies [18, 19]. Despite the consensus white paper recommendation [3] of a 1500 ms PLD for pediatric populations, our results suggest that this may be insufficient for capturing the CBF signal in WM, given the $PCASL_{7PLD}$ ATT value of 1.57 s. These findings support the need to further refine ASL sequence parameters for pediatric cohorts, with the goal of improving regional perfusion quantification and standardization in future studies. Our study found age-related variations between GM and WM. WM CBF decreased with age and increasing WM volume, while the trend was significantly different for GM, with no significant correlation between age and GM volume.

Although age-related declines in WM [20] and GM [21–23] CBF after peaking at 7–10 years have been reported in previous studies, our cohort showed no significant negative linear correlation between GM-CBF and age. Instead, we only observed a negative linear correlation in WM, with significantly divergent trends between GM and WM, as seen in all ASL variants. One possible explanation for this discrepancy from previous studies is the use of a linear regression model across all age groups. Another factor could be the confounding effect of age-related increases in GM-ATT, which we addressed by using multi-PLD PCASL, unlike prior studies that used single-delay PCASL or PASL. Additionally, we excluded the cerebellum from the GM analysis

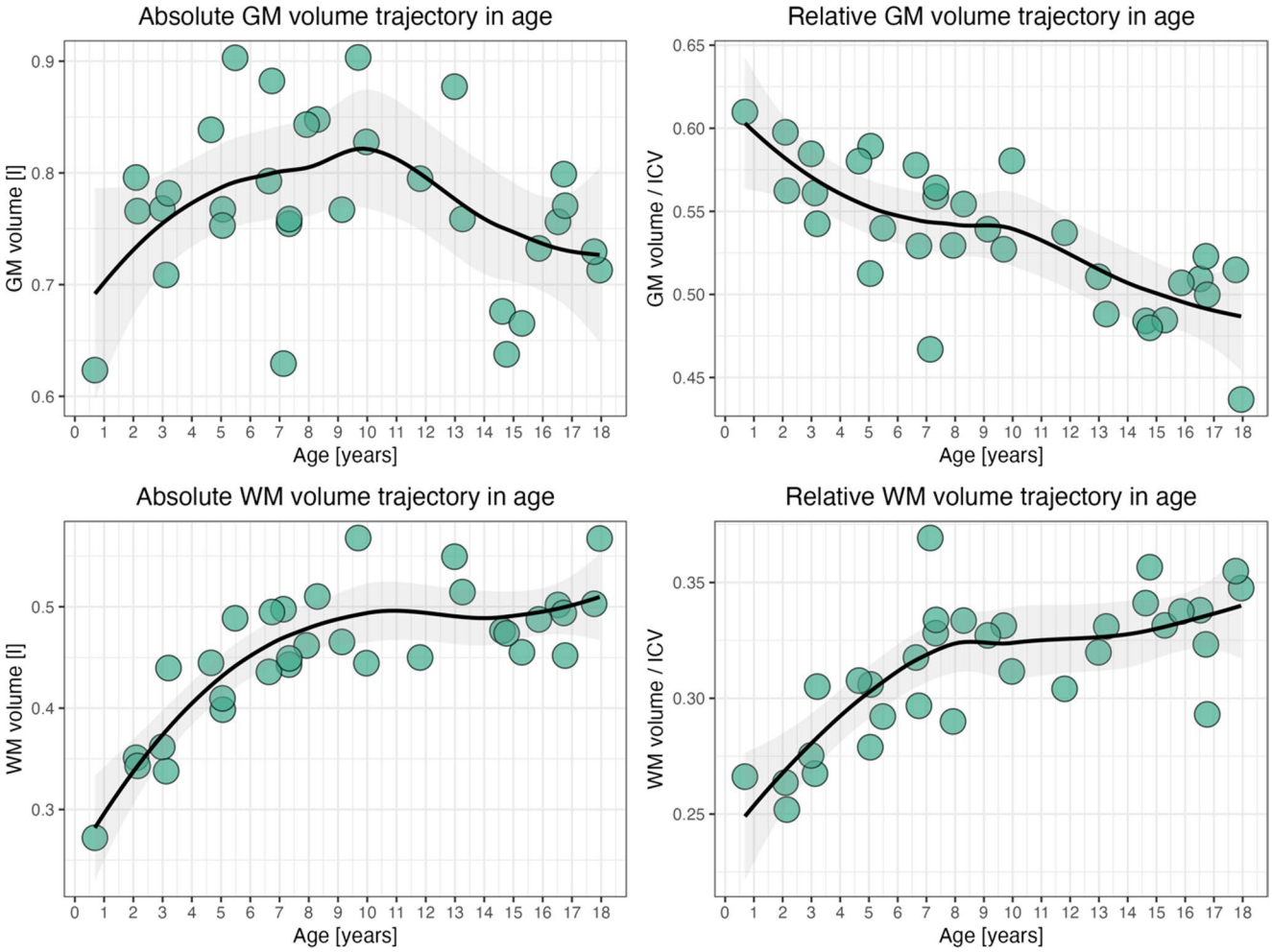

Fig. 6 Absolute and relative GM and WM volume trends in age

Table 4 Correlation analysis of WM and GM volumes with age and regional CBF

	Absolute GM volume	GM ICV ratio	Absolute WM volume	WM ICV ratio	Absolute GM + WM volume	GM + WM ICV ratio
Age	rho = −0.13, p = 0.46	**rho = −0.75, p < 0.001***	**rho = 0.72, p < 0.001***	**rho = 0.71, p < 0.001***	**rho = 0.36, p = 0.046**	rho = 0.26, p = 0.15
$PCASL_{ATC-3PLD}$ GM CBF	rho = −0.34, p = 0.057	rho = 0.10, p = 0.59				
$PCASL_{ATC-3PLD}$ WM CBF			**rho = −0.42, p = 0.02**	**rho = −0.36, p = 0.046**		
$PCASL_{ATC-3PLD}$ TB CBF					**rho = −0.46, p = 0.008***	rho = 0.08, p = 0.68

Highlighted in bold are results with $p < 0.05$

"*" indicates p-values < 0.05 after FWER correction. rho – Spearman rank correlation coefficient

due to its considerable confounding effect, as shown in Supplementary Fig. 2.

We identified a significant positive correlation between age and GM-ATT, but not between age and WM-ATT. The absence of a correlation in WM may be due to the low signal-to-noise ratio typically observed in WM ASL. Interestingly, both CBF and ATT analyses revealed significant age-related trends in the cerebellum, highlighting the need for further investigation of regional hemodynamic changes. Previous studies have shown that cerebellar development

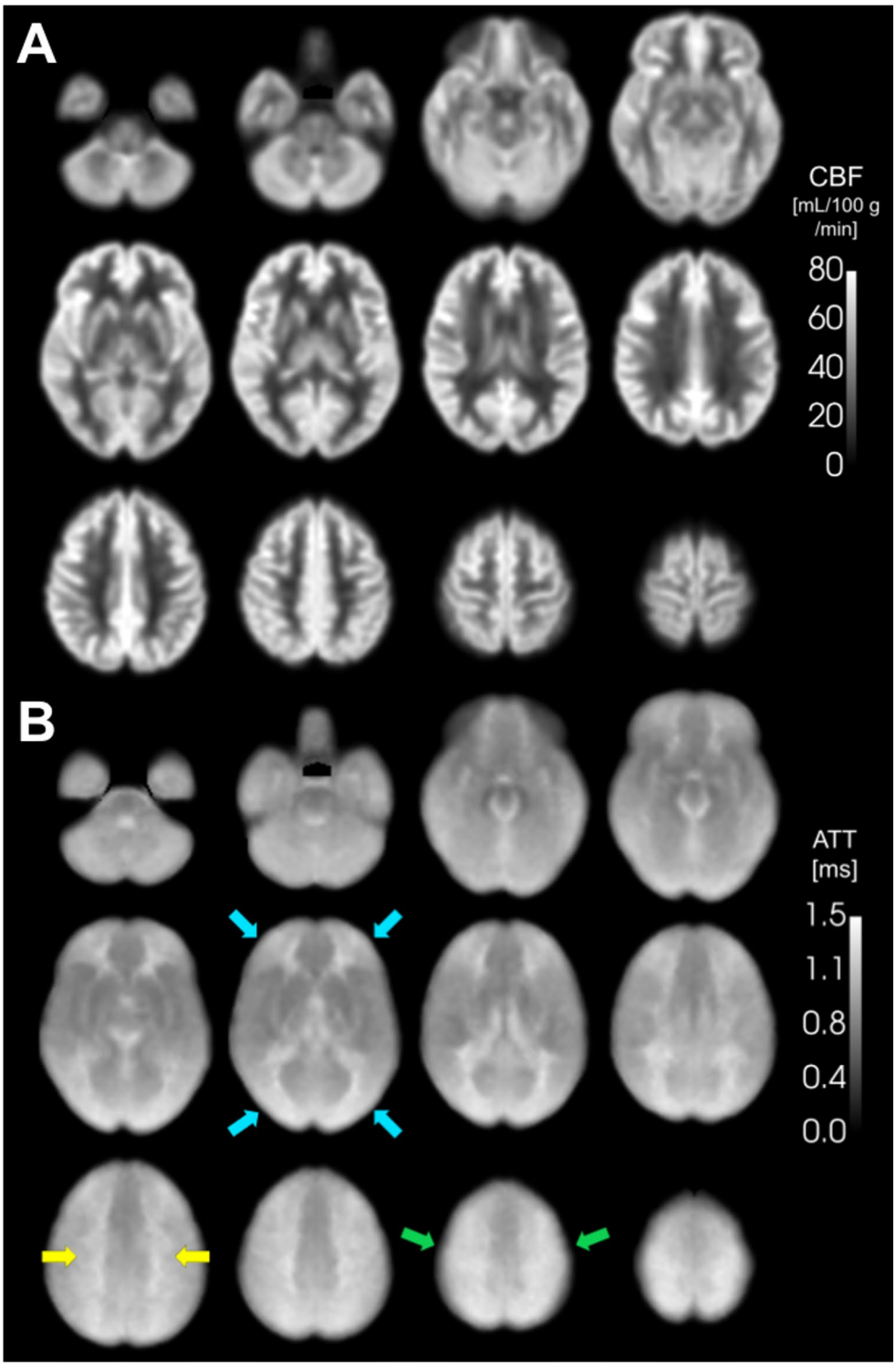

Fig. 7 Population-averaged $PCASL_{3PLD}$ CBF (**A**) and ATT (**B**) images. Blue arrows (middle row, second from left) indicate watershed regions with elevated ATT. Yellow arrows (bottom row, first on the left) highlight areas of deep white matter with elevated ATT. Green arrows (bottom row, third from left) point to regions of elevated ATT in superior brain areas

in children follows a distinct trajectory compared to the cerebrum, with structural maturation completing later and cerebellar volume peaking after cortical regions [24, 25]. To specifically isolate the effects of cortical versus cerebellar contributions to hemodynamic trends, we excluded the cerebellum from the primary analysis. Nonetheless, these findings underscore the importance of future research focusing on cerebellar hemodynamics in pediatric populations.

Moreover, volumetric analysis offers key insights into the differential development of WM and GM in children.

GM-CBF was independent of absolute GM volume, which exhibited no linear correlation with age, consistent with previous studies reporting an inverted U-shaped relationship [26–28]. In contrast, both absolute and relative WM volumes positively correlated with age and were inversely related to WM-CBF changes. Considering the documented decline in total CBF starting at age four [22], these findings shed light on distinct developmental patterns in WM and GM perfusion. Additionally, the population CBF CoV map visually highlights a contrast in hemodynamic variability between WM and GM, with WM exhibiting significantly greater CBF variance in the pediatric cohort compared to GM. These findings underscore the complex interplay between perfusion and brain maturation, with potential implications for pediatric neuroimaging protocols.

Limitations

Sex and sedation are well-established factors influencing pediatric cerebral hemodynamics [29, 30]. Our results demonstrate different age-related trends in mean GM CBF between male and female participants, as illustrated in Supplementary Fig. 2. This finding aligns with the observations of Satterthwaite et al. [8], who reported that puberty and sex-specific developmental trajectories critically shape the evolution of cerebral perfusion during adolescence, with females typically exhibiting increased CBF after pubertal onset, whereas males show a relative decline. Larger cohort studies are needed to establish sex-related trajectories in hemodynamics in pediatric cohorts. Additionally, no significant differences were observed between sedated and non-sedated groups, as the effects of sedation remain inconclusive [7]. Larger cohort studies could explore the effects of different sedation types and levels on pediatric perfusion metrics. Hemodynamic parameters were analyzed across the entire cohort to account for the non-linear relationship between age and cerebral perfusion [21]. Despite not performing age-specific analyses, we observed significant correlations between age and WM-CBF or GM-ATT, providing valuable insights for ASL standardization in pediatric populations and warranting further investigation. Alternative ASL post-processing methods, such as FSL BASIL [31], which incorporates Bayesian modeling and arterial blood volume correction to minimize bias from elevated vascular signal in PWIs acquired with short PLDs, may be valuable for future studies. However, its reliance on parameter initialization is challenging, particularly in pediatric cohorts where such values have yet to be well established. Hence, we used the scanner reconstruction, which applies a nonlinear least-square curve fitting to a perfusion kinetic model [17]. This approach provided a robust and clinically applicable framework for the initial investigation of ATT and CBF. Although common pitfalls in ASL data analysis were carefully addressed in this study, CBF measurement was not validated against gold-standard modalities such as O15-water PET or other contrast agent-dependent methods, due to the ethical and safety concerns associated with exposing pediatric subjects to these procedures. Instead, ASL with three delays was used as a reference for all comparisons, as this sequence was acquired for every participant according to the study protocol. We acknowledge that our approach does not represent a true gold standard, because potential imbalances in age, sex, and sedation across cohorts scanned with different sequences may serve as confounding factors. However, our sensitivity analysis did not reveal any significant differences. However, it has been demonstrated that multi-PLD PCASL achieved a high and strong correlation in CBF measurements with PET in normal and affected brain regions, at least in adults [32]. Additionally, this study's single-center, single-vendor design may limit its generalizability, and further research is warranted to validate these findings against established reference standards, incorporate age-specific developmental modeling, and confirm applicability across multi-center, multi-vendor settings.

Conclusion

This study is the first to directly compare multi-delay and single-delay ASL and report ATT in MR-negative pediatric subjects. Our findings demonstrate the need for careful interpretation of single-delay ASL in children and emphasize the importance of selecting an appropriate PLD for accurate CBF quantification. Future studies on regional cerebral perfusion trends may help further investigate developmental dynamics in typically-developing children.

Supplementary Information The online version contains supplementary material available at https://doi.org/10.1007/s00234-025-03794-9.

Author contributions Y.P., M.Z., E.T., M.M., and R.D.A. contributed to the conceptualization of the study. The analysis was implemented by Y.P., J.P., and M.Z. Data quality control was performed by R.D.A., J.P., and Y.P. Data management was handled by S.A. and Y.P. The original draft was prepared by Y.P., M.Z., and S.A. M.M., G.S., E.T., J.O., M.K., and K.W.Y. provided valuable feedback and comments. All authors contributed to revising the manuscript and approved the final version.

Funding This work was supported by the American Heart Association (Grant No. 23SCEFIA1141920) and the Stanford Maternal and Child Health Research Institute Pilot Grant. The project received additional funding from the Ministry of Education, Youth and Sports of the Czech Republic (Project No. LX22NPO5107), financed by the European Union – Next Generation EU, the Czech Health Research Council (Grant No. NU23-08-00460), the European Union's Horizon Widera programme under grant agreement no. 101159624 (TACTIX), and from the EU Joint Program for Neurodegenerative Disease Research,

provided by the Netherlands Organisation for Health Research and Development and Alzheimer Nederland (DEBBIE JPND2000-568-106). One of the authors was supported by the Luso-American Development Foundation (Grant No. 2020/A-210498). Additional support was provided by the ISMRM Exchange Grant.

Data availability The research data supporting this study can be made available upon reasonable request. Interested researchers may contact the Corresponding Author to obtain further details regarding data access.

Declarations

Ethics approval The study was conducted in accordance with the Declaration of Helsinki [10]. All methods were performed in accordance with the relevant guidelines and regulations.

Consent to participate Written informed consent for secondary data use in the present study was obtained from the parents or guardians of all participants.

Consent to publish Written informed consent to publish secondary data in the present study was obtained from the parents or guardians of all participants.

Competing interests The authors declare no competing interests.

References

1. Vernooij MW, van der Lugt A, Ikram MA et al (2008) Total cerebral blood flow and total brain perfusion in the general population: the Rotterdam scan study. J Cereb Blood Flow Metab 28:412–419
2. Starekova J, Pirasteh A, Reeder SB (2024) Update on Gadolinium-based contrast agent safety, from the AJR special series on contrast media. AJR Am J Roentgenol 223:e2330036
3. Alsop DC, Detre JA, Golay X et al (2015) Recommended implementation of arterial spin-labeled perfusion MRI for clinical applications: a consensus of the ISMRM perfusion study group and the European consortium for ASL in dementia. Magn Reson Med 73:102–116
4. Lindner T, Bolar DS, Achten E (2023) Current state and guidance on arterial spin labeling perfusion MRI in clinical neuroimaging. Magn Reson Med 89:2024–2047
5. Golay X, Ho M-L (2022) Multidelay ASL of the pediatric brain. Br J Radiol 95:20220034
6. Hernandez-Garcia L, Aramendía-Vidaurreta V, Bolar DS et al (2022) Recent Technical Developments in ASL: A Review of the State of the Art. Magn Reson Med 88(5):2021–2042. https://doi.org/10.1002/mrm.29381
7. Zhao MY, Tong E, Duarte Armindo R et al (2024) Measuring quantitative cerebral blood flow in healthy children: a systematic review of neuroimaging techniques. J Magn Reson Imaging 59:70–81
8. Satterthwaite TD (2014) Impact of puberty on the evolution of cerebral perfusion during adolescence. Proc Natl Acad Sci U S A 111(23):8643–8648
9. Faraco CC, Strother MK, Dethrage LM et al (2015) Dual echo vessel-encoded ASL for simultaneous BOLD and CBF reactivity assessment in patients with ischemic cerebrovascular disease. Magn Reson Med 73:1579–1592
10. World Medical Association (2013) World medical association declaration of helsinki: ethical principles for medical research involving human subjects. JAMA 310:2191–2194
11. Dai W, Shankaranarayanan A, Alsop DC (2013) Volumetric measurement of perfusion and arterial transit delay using Hadamard encoded continuous arterial spin labeling. Magn Reson Med 69:1014–1022
12. Mutsaerts HJMM, Petr J, Groot P et al (2020) ExploreASL: an image processing pipeline for multi-center ASL perfusion MRI studies. Neuroimage 219:117031
13. Prysiazhniuk Y, Server A, Leske H et al (2024) Diffuse glioma molecular profiling with arterial spin labeling and dynamic susceptibility contrast perfusion MRI: a comparative study. Neuro-Oncology Advances 6:vdae113
14. Gaser C (2009) Partial volume segmentation with adaptive maximum a posteriori (MAP) approach. *NeuroImage* ; 47:S121. [*Organization for Human Brain Mapping 2009 Annual Meeting*]
15. Holm S (1979) A simple sequentially rejective multiple test procedure. Scand J Stat 6:65–70
16. Chiron C, Raynaud C, Mazière B et al (1992) Changes in regional cerebral blood flow during brain maturation in children and adolescents. J Nucl Med 33:696–703
17. Dai W, Robson PM, Shankaranarayanan A, Alsop DC (2012) Reduced resolution transit delay prescan for quantitative continuous arterial spin labeling perfusion imaging. Magn Reson Med 67:1252–1265
18. van Gelderen P, de Zwart Ja, Duyn Jh (2008) Pittfalls of MRI measurement of white matter perfusion based on arterial spin labeling. Magn Reson Med 59:788–795
19. van Osch MJ, Teeuwisse WM, Chen Z, Suzuki Y, Helle M, Schmid S (2018) Advances in arterial spin labelling MRI methods for measuring perfusion and collateral flow. J Cereb Blood Flow Metab 38:1461–1480
20. Leung J (2016) Developmental trajectories of cerebrovascular reactivity in healthy children and young adults assessed with magnetic resonance imaging. J Physiol 594:2681–2689
21. Carsin-Vu A, Corouge I, Commowick O et al (2018) Measurement of pediatric regional cerebral blood flow from 6 months to 15 years of age in a clinical population. Eur J Radiol 101:38–44
22. Wu C, Honarmand AR, Schnell S (2016) Age-related changes of normal cerebral and cardiac blood flow in children and adults aged 7 months to 61 years. J Am Heart Assoc 5:e002657
23. Taki Y (2011) Correlation between gray matter density-adjusted brain perfusion and age using brain MR images of 202 healthy children. Hum Brain Mapp 32:1973–1985
24. Gaiser C (2024) Population-wide cerebellar growth models of children and adolescents. Nat Commun 15(1):2351
25. Tiemeier H et al (2010) Cerebellum development during childhood and adolescence: a longitudinal morphometric MRI study. Neuroimage 49(1):63–70

26. Morel B, Piredda GF, Cottier J-P et al (2021) Normal volumetric and T1 relaxation time values at 1.5 T in segmented pediatric brain MRI using a MP2RAGE acquisition. Eur Radiol 31:1505–1516
27. Wilke M, Krägeloh-Mann I, Holland SK (2007) Global and local development of Gray and white matter volume in normal children and adolescents. Exp Brain Res 178:296–307
28. Giedd JN et al (1999) Brain development during childhood and adolescence: a longitudinal MRI study. Nature neuroscience 2(10):861–863
29. Makki MI, O'Gorman RL, Buhler P (2019) Total cerebrovascular blood flow and whole brain perfusion in children sedated using propofol with or without ketamine at induction: an investigation with 2D-cine PC and ASL. J Magn Reson Imaging 50:1433–1440
30. Liu Y (2012) Arterial spin labeling MRI study of age and gender effects on brain perfusion hemodynamics. Magn Reson Med 68:912–922
31. Chappell MA, Kirk TF, Craig MS et al (2023) BASIL: A toolbox for perfusion quantification using arterial spin labelling. Imaging Neurosci 1:1–16
32. Zhao MY, Fan AP, Chen DY-T et al (2022) Using arterial spin labeling to measure cerebrovascular reactivity in Moyamoya disease: insights from simultaneous PET/MRI. J Cereb Blood Flow Metab Off J Int Soc Cereb Blood Flow Metab 42:1493–1506

Authors and Affiliations

Yeva Prysiazhniuk[1,2] · Rui Duarte Armindo[3] · Sasha Alexander[4] · Michael Moseley[5] · Kristen W. Yeom[4] · Jakub Otáhal[1] · Martin Kynčl[2] · Elizabeth Tong[5] · Jan Petr[6,7] · Moss Y. Zhao[4] · Gary K. Steinberg[4]

✉ Gary K. Steinberg
cerebral@stanford.edu

Yeva Prysiazhniuk
yeva.prysiazhniuk@lfmotol.cuni.cz

Rui Duarte Armindo
ruimigueldarmindo@gmail.com

Sasha Alexander
sashalex@stanford.edu

Michael Moseley
moseley@stanford.edu

Kristen W. Yeom
kyeom@stanford.edu

Jakub Otáhal
jakub.otahal@lfmotol.cuni.cz

Martin Kynčl
martin.kyncl@fnmotol.cz

Elizabeth Tong
liztong@gmail.com

Jan Petr
j.petr@hzdr.de

Moss Y. Zhao
mosszhao@stanford.edu

[1] Department of Pathophysiology, the Second Faculty of Medicine, Charles University, Prague, Czech Republic

[2] Department of Radiology, Second Faculty of Medicine, Charles University and University Hospital Motol, Prague, Czech Republic

[3] Department of Neuroradiology, Western Lisbon Hospital Centre, Lisbon, Portugal

[4] Department of Neurosurgery, Stanford University, Stanford, CA, United States

[5] Department of Radiology, Stanford University, Stanford, CA, United States

[6] Helmholtz-Zentrum Dresden-Rossendorf, Institute of Radiopharmaceutical Cancer Research, Dresden, Germany

[7] Department of Radiology and Nuclear Medicine, Amsterdam Neuroscience, Amsterdam University Medical Center, Location VUmc, Amsterdam, Netherlands